8-13 MICRON SPECTROSCOPY OF YOUNGSTERS

M.S. Hanner and T.Y. Brooke
MS 183-501, Jet Propulsion Laboratory
California Institute of Technology
4800 Oak Grove Drive
Pasadena CA911 09

and

A.T. Tokunaga
Institute for Astronomy
University of Hawaii
2680 Woodlawn Drive
Honolulu HI 96822

October 1997

Received: ____________________

ABSTRACT

We present 8-13 μm spectra of 23 young stars acquired with the UKIRT CGS3 spectrometer, including T Tauri, Herbig Ae/Be, and FU Ori stars. Silicate emission and absorption features can generally be matched with the Trapezium emissivity, by employing simple models to account for optical depth effects. Two Herbig Ae/Be objects, Lk Hα 208 and Lk Hα 198, have emission features that peak at 9.3 pm. These spectra can be adequately fit with the Trapezium emissivity and a variable optical depth model, plus a hydrocarbon component. A different emissivity peaking at shorter wavelength is not ruled out; however, it is not a *necessary* conclusion from the observed spectra. Two absorption sources appear to require a narrower emissivity profile. The 11.2 μm peak of crystalline olivine observed in comets is not seen in our YSO spectra, to a limit of 5°/0 for emission sources and 15°/0 for absorption profiles.

Aromatic hydrocarbon emission is frequently present in our sample of Herbig Ae/Be stars and is also seen in the T Tauri stars SU Aur (G2 III) and DK Tau (K7). Five objects were observed at higher spectral resolution (R-200) to search for spectral structure in the 11 μm region; the aromatic hydrocarbon band at 11.2pm is resolved into two components at 11.22 and 11.06 μm in Lk Hα 198 and SU Aur.

Subject headings: Infrared: Spectra; Stars: T Tauri;
Stars: Herbig Ae/Be; Stars: YSOS

1. INTRODUCTION

The spectral shape of the 10 μm silicate feature is indicative of the mineralogy and degree of crystallinity of the silicate grains. Silicate grains in molecular clouds such as the Trapezium region exhibit a rather broad, smooth 10 μm feature peaking near 9.7 pm, leading to the conclusion that the grains are glassy or amorphous rather than crystalline (e.g. Day 1974; Dorschner et al. 1988). In contrast, Comet Halley (Bregman et al. 1987, Campins & Ryan 1989) and several new and long period comets, including Hale-Bopp (Crovisier et al. 1997; Hayward & Hanner 1997; Russell & Lynch 1996), display the spectral peak of crystalline olivine at 11.2 μm (see Harmer, Lynch, and Russell 1994 for a review). If comets formed from essentially unaltered interstellar material in the cold outer solar nebula, then the presence of crystalline grains in comets, but not in molecular cloud dust, is surprising.

Young stellar objects represent the transition between molecular cloud dust and the dust which would have been incorporated into comets in the solar nebula. Spectra published to date for young stellar objects with silicate features are generally consistent with the smooth Trapezium emission feature (Cohen & Witteborn 1985, Hanner, Brooke, & Tokunaga 1995, hereafter Paper 1). However, Knacke et al. (1993) found that the 10 μm spectrum of the dust surrounding the young A5V star β Pictoris resembles the comet spectra.

Recently, very clear evidence of crystalline olivine has been detected in HD 100546, a star with strong dust emission and of early spectral type similar to β Pie. Spectra from the Infrared Space Observatory show not only an 11.2 μm peak, but also several strong features due to olivine at 19-34 μm (Waelkens et al. 1996). HD 100546 appears to be a late-stage Herbig Ae/Be star in transition to a β Pie-type object (Grady et al. 1997). In part, this paper attempts to search for more sources such as HD1 00546.

In this paper, we present ground-based low resolution 8-13 μm spectra of 23 young stars. These stars cover a range of spectral types, including T Tauri, Herbig Ae/Be and FU Ori objects. Our objective is to ascertain the spectral shape of the silicate emission and absorption features in these young stars, to extend the survey we began in Paper 1, and to seek compositional links between comets and young stars. Since variations in optical depth, temperature, and amount of intervening' material can affect the spectral shape, simple models based on the Trapezium emissivity are applied, then the spectra are examined for deviations from the Trapezium emissivity. To search for spectral structure in the 11 μm region, several stars were observed at higher spectral resolution.

2. OBSERVATIONS

The 8- 13 μm spectra were taken primarily on UT 1993 November 4-6 at the United Kingdom Infrared Telescope using the CGS3 32-element grating spectrometer in the low resolution (R - 55) and high resolution (R - 190) modes. The aperture size was 3.4 arcsec and the chopping throw was 20 arcsec EW. Two grating positions, spaced approximately 1/2 resolution element apart, were used for the low resolution spectra and 3 grating positions for the high resolution spectra.

The primary calibration star was α Tau. The flux and spectral shape of α Tau at R -55 were calibrated versus Sirius, Sirius was assumed to have a color temperature of 10,000 K and absolute flux density of 4.33x 10^{-12} $W/m^2/\mu m$ at 10.1 pm. The flux density of α Tau, convolved with the N filter bandpass, is consistent with an N magnitude of -3.03 (Tokunaga 1984). Gamma Aql was used as the standard for the sources in Cygnus on Nov. 6 and β Peg for the Cygnus sources on Nov. 4; their spectra were calibrated versus α Lyr during a previous CGS3 run in 1991. A krypton lamp observed through a K filter at fourth, fifth, and sixth orders provided the wavelength calibration. The wavelength scale was verified by observing the planetary nebula NGC 7027; we estimate the wavelength uncertainty to be ± 0.02 pm.

We include two sources, Elias 1-12 and V536 Aql, which were observed with CGS3 on UT 1992 June 24, using a 4.8 arcsec aperture and 20 arcsec EW throw. The calibration stars were α Lyr and β Peg.

Table 1 summarizes the observed sources. These include a sample of Herbig Ae/Be stars, T Tauri stars, and FU Ori objects. Several of these sources were selected from the objects observed by Cohen&Witteborn(1985) because they showed the possibility of interesting spectral structure in the silicate feature.

3. THE SILICATE FEATURES

The low resolution 7.8- 13.4 μm spectra are presented in Fig. 1-3 for the Herbig Ae/Be stars, T Tau stars, and FU Ori objects respectively. It is not possible to derive uniquely the spectral emissivity of the silicate grains without knowing the densities, temperatures, and geometry of the dust population. Following Paper 1, we have fit the spectra with the simple models described below, in order to determine approximate optical depths and to ascertain whether the Trapezium emissivity can adequately represent the observed spectral shapes. We use the Trapezium emissivity derived in Paper I from our CGS3 spectra of θ^1 Ori D. Emission features were modeled for cases 1-2 and absorption features with cases 3 and 4. For each case, a least squares minimization was performed to determine the best-fit values for the optical depth, spectral index, and normalization factors. The resulting best-fit parameters are given in Tables 2 and 3. For the emission sources, the dashed line in the figures refers to the best fit for Case 1, variable optical depth, and the solid line to the best fit for Case 2, two components. For the absorption sources, the solid lines are for Case 4 and the dashed lines for Case 3. We have included an empirical fit to the 7.7, 8.6, and 11.25 μm hydrocarbon bands in our models for Lk Hα 198, Lk Hα 208, and SU Aur, following the procedure described in Paper 1. The parameter a_c in Table 2 is the contribution of the hydrocarbon component at 11.1 pm.

Case 1- Variable optical depth (after Cohen and Witteborn 1985)

$$\lambda F_{\lambda} = a_0\left(\frac{\lambda}{9.7}\right)^m \left(1 - e^{-a_1\varepsilon_t(\lambda)}\right) \qquad (1)$$

With $\varepsilon_t(\lambda)$ normalized at 9.7 pm, the parameter a_1 *is* the total silicate optical depth at 9.7 μm, $\tau_{9.7}$. This slab model approximates a dusty envelope which both emits and absorbs at 10 μm.

Case 2- Two **component: Optically thick+ optically thin emission**

$$\lambda F_{\lambda} = a_0\left(\frac{\lambda}{9.7}\right)^n + a_2\left(\frac{\lambda}{9.7}\right)^m \varepsilon_t(\lambda) \qquad (2)$$

The quantity $f = a_2/(a_0 + a_2)$ *is* the relative contribution of the optically thin grains to the flux at 9.7 pm. This model might apply, for example, to an optically thin envelope and an optically thick disk (or the star itself), both of which contribute to the flux at 10 pm. The optically thick component could alternatively represent emission from featureless dust,

Case 3- **Optically thin with line of sight extinction** (after Gillett et *al.* 1975)

$$\lambda F_{\lambda} = a_0\left(\frac{\lambda}{9.7}\right)^m \varepsilon_t(\lambda) e^{-a_1\varepsilon_t(\lambda)} \qquad (3)$$

The parameter a_1 is equal to the total line of sight extinction by non-emitting grains at 9.7 pm, $\tau_{9.7}$. Note that both the emitting and the absorbing grains are assumed to have the Trapezium emissivity. This equation might apply to an optically thin circumstellar envelope obscured by cold dust along the line of sight.

Case 4- Optically thick with line of sight extinction

$$\lambda F_\lambda = a_0 (\frac{\lambda}{9.7})^m \, e^{-a_1 \varepsilon_t(\lambda)} \qquad \textbf{(4)}$$

This equation might apply to an optically thick disk or envelope (or the star itself) obscured by cold dust.

Clearly, the geometry of the dust cloud and the optical depth affect the width and shape of the silicate feature, as can be seen by comparing the model fits to the various spectra.

Herbig Ae/Be Stars

The Herbig Ae/Be stars are pre-main sequence stars of early spectral type (Thé et al, 1994). These objects display a variety of 10 μm spectra. The emission spectrum of WW Vul closely resembles the width and peak position of the T Tauri star DI Cep; both are well matched with the Trapezium emissivity profile. Consistency with the Trapezium emissivity does not require the observed spectrum to peak at 9.7 μm. The best example is Lk Hα 208, where the observed emission profile peaks at 9.3 pm. This source can be adequately fit with a variable optical depth model (Case 1) plus an aromatic hydrocarbon component. Other examples are Lk Hα 198 and the Herbig Ae/Be star HD 150193 in the ρ Ophiuchi cloud (Paper 1). A different emissivity peaking at shorter wavelength than the Trapezium is also possible, but is not a *necessary* conclusion from the observed profiles in our sample.

Lk Hα 198 and V376 Cas are the most prominent visible stars in a small isolated molecular cloud. V376 Cas has the largest linear polarization yet observed in a young stellar object; the elongated structure indicates we are seeing an edge-on disk (Asselin et al. 1996). The increase in polarization towards longer λ implies that the grains are larger than typical interstellar grains. V376 Cas appears to be an example of silicate self-absorption, which we modeled by

$$\lambda F_\lambda = (a_0 \, (\frac{\lambda}{9.7})^n + a_1 \, (\frac{\lambda}{9.7})^m \, (1 - e \text{ ‘a’ } \epsilon_t \text{ ‘a’})) \,) \, e^{-a_4 \epsilon_t(\lambda)}$$

with a_0 = 25.37, n=-1 .87, a_1=412., m=O.42, a_3=0.407, a_4=0.955.

T Tauri stars

The silicate emission sources in our small sample of T Tauri stars are consistent with the Trapezium emissivity, within the error bars. Two of the stars with silicate absorption features, T Tau and Haro 6-10, have known companions which were included in our 3.4 arcsec aperture (Table 1) and have been detected previously in the 10 μm region (Ghez et al. 1991, van Cleve et al. 1994). T Tau N is an optically visible star, while T Tau S is a variable embedded infrared source. The 1990 data for T Tau N from Ghez et al. were scaled to the van Cleve et al. data which were taken Nov 14, 1992, closer in time to our CGS3 spectrum. The filter photometry of T Tau N and Haro 6-10 S was fit with an optically thick plus optically thin emission model (Case 2), assuming the Trapezium emissivity, and the fits were subtracted from the CGS3 spectra, as shown in Figure 4. Haro 6-10 S was indistinguishable from a power law. The resulting spectra of T Tau S and Haro 6-10 N were then fit with the silicate absorption model (Case 4); models with emission plus absorption (Case 3) provided poorer fits and are not shown. Because the companions, T Tau N and Haro 6-10 S, have relatively flat spectra, the shapes of the absorption profiles are not strongly affected by the presence of the companion. Recent spatially resolved photometry in August 1996 (Herbst et al. 1997) is in good agreement with our derived spectrum of T Tau N. Their fluxes for T Tau S are ~60% of our fluxes, confirming the strong variability of T Tau S.

The spectra of T Tau S, Haro 6-10 N, as well as HL Tau, appear to require a narrower emissivity than the Trapezium. Their shapes are similar to those seen in two deep absorption profiles of protostars in ρ Ophiuchi (Paper 1). Figure 5 displays the emissivity derived by inverting the fit to T Tau S, following the procedure described in Paper 1; it is very close to that derived previously for Elias21. One possible explanation is that the grains are smaller toward these sources than in the Trapezium region; compositional differences are also a possibility (Jäger et al. 1994). Our conclusion that the silicate absorption feature toward T Tau S is narrower than the Trapezium disagrees with the conclusion of Herbst et al. based on the inverted profile from their filter photometry alone.

FU Ori Stars

The FU Ori stars are pre-main sequence stars of optical spectral type late F to G, which undergo brightness outbursts thought to be due to sudden increases in mass accretion. Of the 9 objects in the review of Hartmann and Kenyon (1996), 10 μm spectra of 4 are given here. Another, Z CMa, was observed by Cohen and Witteborn (1985). It has a shallow silicate absorption feature well-matched by the Trapezium profile. L 1551-IRS 5 also has a silicate absorption feature (Cohen and Schwartz 1983), though the profile is not well-determined,

There are two things to note about the FU Ori silicate features. First, all of the features appear to be compatible with the Trapezium profile. Second, none of the FU Ori stars observed to date show a strong silicate emission feature. Three of the six show weak silicate emission, while the other 3 show silicate absorption. This distribution is consistent with randomly-oriented objects whose dust envelopes have a solid angle filling factor of order ½ (Hartmann and Kenyon 1996), though the sample is small and regions of silicate emission could fall within the aperture of an edge-on object. Optically thin silicate dust can contribute in the sources with weak emission features (the two component model, Case 2, actually provides good fits to these objects) but it does not dominate the 10pm spectra. This supports models of FU Ori stars which assign most of the 10 μm emission to accretion disks which are optically thick at 10 μm (Kenyon and Hartmann 1991). An alternative model of a dust envelope around V 1057 Cyg (Kenyon and Hartmann 1991) gives too strong a silicate emission feature to match the data at the current epoch.

V 1057 Cyg brightened by 5 mag at visual wavelengths in 1970, and has faded gradually since then (Simon and Joyce 1988). We observed the star in both 1992 and 1993. A possible 11.2 μm feature at the 5% level appears in our June 1992 spectrum, taken with a 4.8 ″ aperture, but is absent in the November 1993 spectrum, taken with a 3.4 ″ aperture, and was not seen in CGS3 data taken in May 1993 (E. L. Jensen, private communication). If the hydrocarbon emission arises from an extended region (e.g. Natta & Krügel 1995), then the difference between our 1992 and 1993 spectra could be due to the difference in beam size.

Upper Limit to Crystalline Olivine

Calculations were made using the model parameters from Tables 2 & 3 and the computed emissivity for a mixture of crystalline and amorphous olivine tetrahedral (Yanamandra-Fisher & Hanner 1997) in order to establish an upper limit to the fraction of crystalline olivine present in the observed sources. For the emission sources (Case 1), 10°/0 crystalline olivine gives a broad shallow feature at the 10% level and even 5% olivine a shallow bump at the 5% level. Discrimination between crystalline olivine and the 11.25pm hydrocarbon band has to be based on higher resolution (R-200) spectra and/or the presence of the other hydrocarbon bands. On the basis of our analysis in Section 4, we conclude that the observed 11.2pm emission excess in our sources is primarily caused by aromatic hydrocarbon emission and the upper limit to crystalline olivine is, at most, a few percent. For the absorption sources (Case 4), 10% crystalline olivine produces a weak signature that could be hidden in the scatter of the data, while a 20% olivine would have produced an observable feature. .

4. THE HYDROCARBON EMISSION BANDS

A number of young stars display the series of emission bands at 3.3,6.2,7.7, 8.6, and 11.2 μm generally attributed to polycyclic aromatic hydrocarbons or aromatic structures in small amorphous grains (Sellgren 1994). Among the 6 Herbig Ae/Be stars we observed, 3 have definite 11.2 μm features at the level of 15- 20%: XY Per, Lk Hα 198, and Lk Hα 208. WW Vul and Lk Hα 233 possibly have a feature < 10'% above the continuum. Of the 8 T Tauri stars with silicate emission, SU Aur and DK Tau show 11.2 μm emission at the 15°/0 level relative to the continuum. A weak feature is possibly present in DI Cep ≤10% above the model flux. None of the T Tauri objects with silicate absorption has an obvious 11.2 μm emission feature.

In low resolution spectra, the 11.2 μm aromatic feature can be confused with the crystalline olivine peak at nearly the same wavelength. The identification rests on the shape of the feature and the presence of the other aromatic bands. For example, Schutte et al. (1990) proposed that the 11.2 μm peak in the Herbig Ae star Elias 1 is due to olivine, whereas Hanner, Brooke & Tokunaga (1994) argued from the CGS3 spectrum at resolution -190 that the shape resembles the aromatic feature, consistent with the presence of the other hydrocarbon bands in this object.

To investigate the 11 μm spectral region, we were able to observe 5 of our objects at resolution R~ 190. These spectra are presented in Figure 6. Lick Hα 198 and SU Aur showed prominent 11.2 μm features. The T Tau star RY Tau has a weak feature, about 6% above the continuum. Neither of the silicate absorption sources, Haro 6-10 nor V645 Cyg, show any emission excess near 11.2 pm.

The Herbig Be star Lick Hα 198 displays an 11.2 μm feature about 10% above the continuum. Both the R-55 and R-1 90 spectra appear to have an emission plateau, or weak overlapping bands, from 10.8 to 11.6 μm. A linear continuum fit at 10.73 and 11.64 -12.0 μm was subtracted from the fluxes in Fig. 6; the resulting excess fluxes are plotted in Figure 7. The feature can be compared to that in the Herbig Ae star Elias 1, which we observed with CGS3 the same night (Hanner et al. 1994). The FWHM, shape, and peak wavelength agree quite well with Elias 1. Within the uncertainties, the shape agrees with the 4 sources presented in Witteborn et al. (1 989), although Lick Hα 198 is somewhat wider on the long-wavelength side. (Abetter match to the width would be obtained if the continuum were fit at 10.98 and 11.5 μm.)

SU Aur is notable in exhibiting an emission feature at 11.2 μm although it has a fairly late spectral type of G2 III (Strom et al. 1989). The high resolution spectrum shows the 11.2 μm feature about 16°/0 above the underlying emission. There is also excess emission at 11.0-11.05 μm, but not as sharply peaked as the 11.06 μm feature in Elias 1, and a possible weak feature near 11.6 pm, also similar to Elias 1. A linear continuum fit at 10.4 -10.9 and 11.7 -12.0 μm was subtracted from the fluxes to give the residual fluxes plotted in Fig. 8. The peak position occurs at -0.05 μm longer wavelength and the FWHM is -0.05 μm wider than the emission profiles of the 4 sources discussed by Witteborn et al. (1989).

All 5 of our Herbig Ae/Be stars with possible 11.2 μm emission were observed by Brooke, Tokunaga, & Strom (1993) in the 3 μm region; the 3.29pm emission band was detected only in XY Per. Brooke et al. found that, of the 41 Herbig Ae/Be stars with 3 μm spectra, about 20% have 3.29 μm emission. While our sources would suggest that the aromatic hydrocarbon bands are more common than that around young stars, our sample was not random, but purposely selected as "interesting" objects. Our detection of 11.2 μm emission in SU Aur (G2) and DK Tau (K7) demonstrates that aromatic hydrocarbon emission is not restricted to early-type stars. This is consistent with Natta & Krügel (1995), who predict that a star of solar luminosity and T~ 5000 K can produce PAH emission bands. There is no hydrocarbon emission detected around the FU Ori stars, with the possible exception of V 1057 Cyg in a 4.8 arcsec beam.

The flux in the 11.2 μm aromatic band in XY Per is 1.1 x 10"14 W/m^2 in a 3.4 arcsec diameter aperture. The 3.3 μm band flux through a 3 arcsec aperture was 3.8 x 10-15 W/m^2 (Brooke et al. 1993). These bands refer to the same functional group in the aromatic structures: the 11,2 μm feature is an out-of-plane C-H bend and the 3.3 μm feature is a C-H stretch. The 3.3/1 1.2 ratio for XY Per is 0.34, in good agreement with that of other Herbig Ae/Be stars (Brooke, Tokunaga, and Strom 1993), including Elias 1. The band ratio cannot be determined for LkHα 198 and LkHα 208 because only upper limits are available for the 3.3 μm fluxes (Brooke et al. 1993), but the upper limits are roughly consistent with the value given above.

5. CONCLUSIONS

We have obtained 8-13 μm spectra of 23 T Tauri, Herbig Ae/Be, and FU Ori stars, in order to investigate the shape of the silicate feature. We find that most sources are compatible with the Trapezium emissivity, when simple models are used to account for optical depth and geometric effects. Two of the Herbig Ae/Be stars, Lk Hα 208 and Lk Hα 198, have emission profiles that peak at 9.3 pm, similar to the Herbig Ae object HD 150193 in the p Ophiuchi cloud (Paper 1). These sources can be adequately fit with the Trapezium emissivity and a variable optical depth model, A different emissivity peaking at shorter wavelength is not ruled out; however, it is not a *necessary* conclusion from the observed spectra. This result emphasizes the importance of taking optical depth effects into account before drawing conclusions about the shape of the emissivity. Two T Tauri absorption sources (T Tau S and HL Tau) have a narrower emissivity profile. Similar narrow emissivity profiles were found for two absorption sources in the p Oph cloud (Paper 1).

We find that aromatic hydrocarbon emission is apparently common around early-type stars and appears in some stars of late spectral type as well.

There is no positive evidence for the 11.2 μm feature of crystalline olivine in any of our sources. In cases where an 11.2 μm bump is present, the shape -- and the presence of related emission bands -- are consistent with the aromatic hydrocarbon feature at 11.22 pm. Given the presence of crystalline olivine in comets, in β Pictoris, and in the transition object HD1 00546 (Waelkens et al. 1996), the lack of evidence for crystalline olivine in young stellar objects is puzzling. Further investigation of these objects is clearly warranted, especially searches for crystalline silicate features in the 18-35 μm spectral region.

We thank the staff of the UKIRT and Joint Astronomy Centre for their support. UKIRT is operated by the Royal Observatory Edinburgh on behalf of the U.K. Science and Engineering Research Council. M. Hanner's research was carried out at the Jet Propulsion Laboratory, California Institute of Technology, under contract with the National Aeronautics and Space Administration. A. Tokunaga acknowledges the support of NSF Grant AST-91 14940.

REFERENCES

Asselin, L., Menard, F., Bastien, P., Monin, J.-L., and Rouan, D. 1996, ApJ, 472,349

Bregman, J. D., Campins, H., Witteborn, F. C., Wooden, D. H., Rank, D. M., Allamondola, L. J., Cohen, M. and Tielens, A. G. G. M. 1987, A&A, 187,616

Brooke, T. Y., Tokunaga, A. T., and Strom, S.E. 1993, AJ, 106,656

Campins, H. & Ryan, E. 1989, ApJ, 341, 1059

Cohen, M. and Schwartz, R.D. 1983, ApJ, 265,877

Cohen, M. & Witteborn, F.C. 1985, ApJ, 294,345

Coulson, I. and Walther, D. 1995, MNRAS, 274,977

Crovisier, J. Leech, K., Bockelee-Morvan, D., Brooke, T. Y., Hanner, M. S., Altieri, B., Keller, H. U., and Lellouch, E. 1997, Science, 275, 1904

Day, K.L. 1974, ApJ, 192, L15

Dorschner, J., Friedemann, C., Gurtler, J. and Henning, T. 1988, A&A, 198,223

Ghez, A. M., Neugebauer, G., Gorham, P. W., Haniff, C. A., Kulkarni, S. R., Matthews, K., Koresko, C. & Beckwith, S. 1991, AJ, 102,2066

Gillett, F. C., Forrest, W. J., Merrill, K. M., Capps, R. W., & Soifer, B.T. 1975, ApJ, 200,609

Grady, C. A., Sitko, M. L., Bjorkman, K. S., Perez, M. R., Lynch, D. K., Russell, R. W., and Hanner, M.S. 1997. ApJ, 483,449

Hanner, M. S., Brooke, T.Y. & Tokunaga, A.T. 1994, ApJ Lett, 433, L97

Hanner, M. S., Brooke, T.Y. & Tokunaga, A.T. 1995, ApJ, 438,250

Hanner, M. S., Lynch, D.K. & Russell, R.W. 1994, ApJ, 425,274

Hartmann, L. and Kenyon, S.J. 1996, Ann. Rev. Astr. Ap, 34,207

Hayward, T.L. & Hanner, M.S. 1997, Science, 275, 1907

Herbst, T. M., Robberto, M. and Beckwith, S. V. W. 1997, AJ, 114,744

J"ager, C., Mutschke, H., Begemann, B., Dorschner, J. & Henning, Th. 1994, A&A, 292,641

Jourdain de Muizon, M., d'Hendecourt, L.B. and Geballe, T.R. 1990, AA, 227,526

Kenyon, S.J. and Hartmann, L.W. 1991, ApJ, 383,664

Knacke, R. F., Fajardo-Acosta, S. B., Telesco, C. M., Hackwell, J. A., Lynch, D.K, and Russell, R.W. 1993, ApJ,418, 440

Natta, A. and Krügel, E. 1995, A&A, 302,849

Puget, J.L. and Le'ger, A. 1989, Ann. Rev. Astr. Ap., 27, 161

Russell, R. W., Lynch, D. K., 1996, IAU Circular 6448

Sandford, S.A. & Walker, R.M. 1985, ApJ, 291,838

Schutte, W. A., Tielens, A. G. G. M., Allamandola, L.J. Cohen, M. & Wooden, D.H. 1990, ApJ, 360, 577

Sellgren, K. 1994, in the First Symposium on the Infrared Cirrus and Diffuse Interstellar Clouds, ASP Conference Series, Vol. 58, ed. R. M. Cutri and W. B. Latter, p. 243

Simon, T. and Joyce, R.R. 1988, PASP, 100, 1549

Stephens, J.R. & Russell, R.W. 1979, ApJ, 228,780

Strom, K. M., Strom, S. E., Edwards, S., Cabrit, S., Skrutskie, M.F. 1989, AJ, 97, 1451

Sylvester, R. J., Skinner, C. J., Barlow, M. J., and Mannings, V. 1996, MNRAS, 279,915

The', P. S., de Winter, D. and Pe'rez, M.R. 1994, AA Suppl., 104,315
Tokunaga, A.T. 1984, AJ, 89, 172
van Cleve, J. E., Hayward, T. L., Miles, J. W., Gull, G. E., Schoenwald, J. and Houck, J.R. 1994, Astr. Sp. Sci., 212,231
Waelkens, C. et al, 1996, AA, 315, L245
Witteborn, F, C., Sandford, S. A., Bregman, J. D., Allamandola, L. J., Cohen, M., Wooden, D.H. & Graps, A.L. 1989, ApJ, 341,270
Yanamandra-Fisher, P. and Hanner, M. S. 1997, submitted to Icarus

TABLE 1

Sources Observed

Source	Date (UT)	Type	Binary Separation / Comments
Lk Hα 198	11/4/93	Herbig B8e	6.″ N
	11/6/93		high res.
V376 Cas	11/4/93	Herbig B5e	
XY Per	11/4/93	Herbig Ae/Be	
Lk Hα 208	11/5/93	Herbig FOe; B7e	0.″115
WW Vul	11/6/93	Herbig A3e	
V645 Cyg	11/6/93	Protostar 07e	
	11/6/93		high res.
Lk Hα 233	11/4/93	Herbig A7e	
V 773 Tau	11/4/93	T Tau	0?17
RY Tau	11/6/93	T Tau	high res.
T Tau	11/5/93	T Tau KO; FUOri	0.″7
DK Tau	11/5/93	T Tau K7	
HL Tau	11/5/93	T Tau K7	
Haro 6-13	11/5/93	T Tau	
HP Tau	11/5/93	T Tau K3	0?02
UY Aur	11/5/93	T Tau K7	0?89
Haro 6-10	11/5/93	T Tau K3	1.″2
	11/6/93		high res.
SU Aur	11/5/93	T Tau G2	
	11/6/93		high res.
V 536 Aql	6/24/92	T Tau	
V 1331 Cyg	11/6/93	T Tau	
DI Cep	11/5/93	T Tau	
FU Ori	11/5/93	FU Ori	
V1515 Cyg	11/4/93	FU Ori	
V1057 Cyg	11/4/93	FU Ori	
	6/23/92		
V1735 Cyg[a]	6/24/92	FU Ori	
Trapezium	11/4/93		
	11/6/93		high res.
0’ D	.1 1/4/93		
	11/6/93		high res.

[a]Elias 1-12

TABLE 2

Fit Parameters for Emission Features

	Case 1				Case 2					Case 3		
	variable optical depth				two components					optically thin with extinction		
Object	a_0^b	m	$\tau_{9.7}$	a_e^b	a_0^b	n	a_2^b	m	a_e^b	a_0^b	m	79.7
T Tauri												
DI Cep	18.7	-0.36	0.40						-	7.4	-0.35	0.17
	(1.4)	(.05)	(.04)							(0.2)	(.05)	(.03)
HP Tau	4.7	-0.62	2.58		1.8	-1.4	2.7	0.6		10.7	-0.64	0.92
	(0.1)	(.04)	(.11)		(0.1)	(0.4)	(0.1)	(0.3)		(0.2)	(.04)	(.03)
DK Tau	6.4	-0.95	2.37	-	2.1	-2.3	4.0	0.6		14.1	-0.97	0.89
	(0.1)	(.04)	(.09)		(0.2)	(0.5)	(0.2)	(0.2)		(0.2)	(.04)	(.02)
UY Aur	5.3	-0.15	4.66		3.4	-0.6	2.0	1.9	-	18.5	-0.20	1.30
	(0.1)	(.05)	(.26)		(0.1)	(0.3)	(0.2)	(0.8)		(0.5)	(.06)	(.04)
V536 Aql	7.0	-0.15	3.10		3.6	-0.05	3.5	-0.03	-	18.6	-0.15	1.03
	(0.2)	(.07)	(.20)		(0.2)	(.34)	(0.3)	(.77)		(0.6)	(.07)”	(.04)
V1331Cyg	2.6	-0.20	2.93		0.8	-3.5	1.7	2.6		6.4	-0.20	0.98
	(0.1)	(.10)	(.26)		(0.2)	(1.8)	(0.2)	(0.2)		(0.3)	(.10)	(.06)
Haro 6-13	3.2	0.26	4.82		1.7	-1.6	1.6	3.7		11.4	0.22	1.32
	(0.1)	(.05)	(.27)		(0.2)	(0.7)	(0.2)	(0.3)		(0.3)	(.05)	(.04)
SU Alu	68.6	-0.47	0.28	1.37	-	-	-	-				
	(13.6)	(.03)	(.02)	(.04)								
FU Ori												
V1057 Cyg	20.9	0.39	5.71		15.0	-0.54	6.3	4.1		78.8	0.37	1.37
	(0.1)	(.01)	(.09)		(0.3)	(.14)	(0.3)	(0.2)		(0.5)	(.01)	(.01)
V1515 Cyg	6.2	-0.10	3.88		3.3	-1.3	3.0	2.6		19.0	-0.13	1.16

	(0.1)	(.03)	(.12)		(0.2)	(0.4)	(0.2)	(0.3)	-	(0.3)	(.03)	(.02)
FU Ori	17.4	-0.87	7.38	-	12.0	-2.0	6.0	2.9	-	72.3	-1.01	1.46
	(0.1)	(.01)	(.15)		(0.3)	(0.2)	(0.3)	(0.1)		(0.4)	(.01)	(.01)
Herbig **Ae/Be**												
WW Vul	17.4	-1.38	0.60	-						10.4	-1.38	0.28
	(2.0)	(.07)	(.09)							(0.3)	(.07)	(.04)
Lk Ha 198	70.3	-0.04	0.82	3.40	6.9	-3.2	33.2	0.99	2.21			
	(1.8)	(.02)	(0.03)	(0.08)	(0.4)	(0.3)	(0.4)	(0.04)	(.10)			
Lk Ha 208	25.8	-0.90	0.71	0.69	1.44	-1.4	12.0	-0.65	0.72			
	(1.8)	(.04)	(.07)	(.06)	(.17)	(0.6)	(0.2)	(.13)	(.06)			

[a]Errors in parentheses
[b]Units are 10^{-13} W m^{-2}

TABLE 3

Fit Parameters for Absorption Features

	Case 3			Case 4		
	optically thin with extinction			optically thick with extinction		
	a_o	m	$\tau_{9.7}$	a_o	m	79.7
T Tauri						
T Tau (S)	501.2	-0.47	2.55	91.9	-0.22	0.73
	(1.9)	(.01)	(.01)	(0.3)	(.01)	(.01)
Haro 6-10 (N)	140.8	1.44	2.73	27.2	1,56	0.96
	(1.8)	(.02)	(.02)	(0.3)	(.02)	(.02)
HL Tau	86.9	-0.11	2.35	16.3	0.14	0.56
	(0.8)	(.02)	(.01)	(0.1)	(.02)	(.01)
FU Ori						
Elias 1-12	27.5	-0.96	1.89	5.33	-0.74	0.13
	(0.9)	(.07)	(.04)	(.17)	(.07)	(.04)
Herbig Ae/Be						
Lk Ha 233	65.4	0.25	1.81	13.0	0.44	0.10
	(0.4)	(.01)	(.01)	(0.1)	(.01)	(.01)
V645 Cyg	1784.5	-0.03	2.20	331.33	0.26	0.42
	(8.8)	(.01)	(.01)	(1.50)	(.01)	(.01)

Figure Legends

Fig, I-(a-i), Spectra of Herbig Ae/Be stars taken with the UKIRT CGS3 low-resolution grating. Model fits are described in the text and are summarized in Tables 2 and 3.

Fig. 2 -(a-1). Spectra of T Tauri stars taken with the UKIRT CGS3 low-resolution grating. Model fits are described in the text and are summarized in Tables 2 and 3. V773 Tau shows neither silicate emission nor silicate absorption.

Fig. 3- (a-e). Spectra of FU Ori stars taken with the UKIRT CGS3 low-resolution grating. Model fits are described in the text and are summarized in Tables 2 and 3. V 1057 Cyg was observed in 1992 and 1993; the model fits were done for the 1993 spectrum.

Fig. 4a. Spectrum of the binary system T Tau. Filled circles: observed CGS3 spectrum of T Tau (N+S); squares: photometry of T Tau N (see text); open circles: spectrum of T Tau S obtained by subtracting the fit to the T Tau N photometry from the observed (N+S) spectrum. The T Tau S spectrum has been fit with a model for Case 4.

Fig. 4b. Spectrum of the binary system Haro 6-10. Filled circles: observed CGS3 spectrum of Haro 6-10 (N-tS); squares: photometry of Haro 6-10 S (see text); open circles: spectrum of Haro 6-10 N obtained by subtracting the power-law fit to Haro 6-10 S. This spectrum has been fit with a Case 4 model.

Fig. 5. Derived emissivity of T Tau S obtained by inverting the fit from the model parameters in Table 3 (filled circles). Dashed line is the emissivity derived for Elias 21 (Paper 1).

Fig. **6-** (a-e). Spectra taken with the UKIRT CGS3 high resolution grating (R-190). Dashed lines are linear fits to the continuum.

Fig. **7.** The 11.2 μm feature in Lk Hα 198. The linear continuum fit at 10.73 μm and 11.64- . 12.0 μm was subtracted from the high-resolution spectrum shown in Fig. 6.

Fig. 8. The 11.2 μm feature in SU Aur after subtracting a linear continuum fit at 10.4 -10.9 μm and 11.7 -12.0 μm.

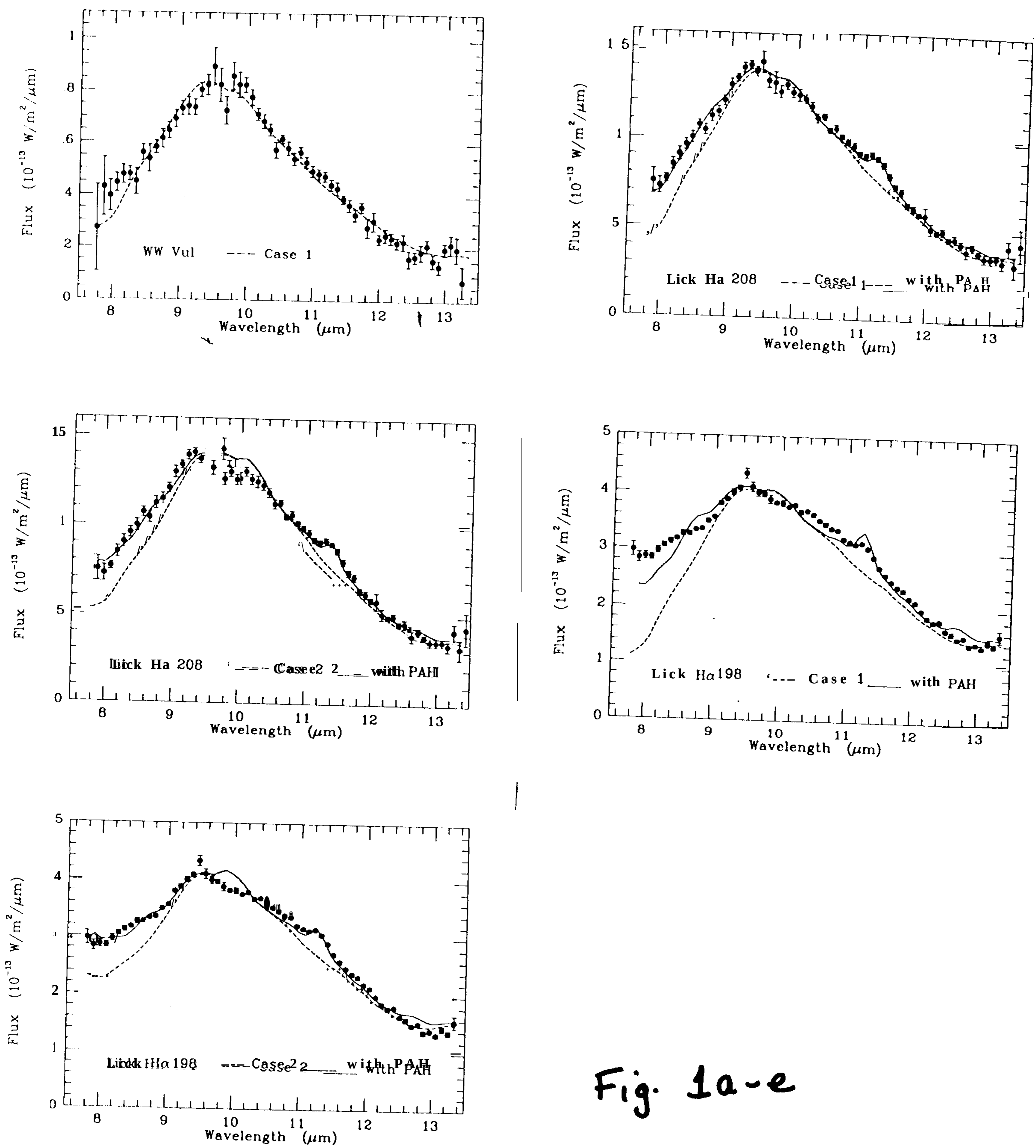
WW Vul --- Case 1
Lick Ha 208 --- Case 1 ___ with PAH
Lick Ha 208 --- Case 2 ___ with PAH
Lick Hα198 --- Case 1 ___ with PAH
Lick Hα 198 --- Case 2 ___ with PAH
Flux (10^{-13} W/m^2/μm)
Wavelength (μm)

Fig. 1a-e

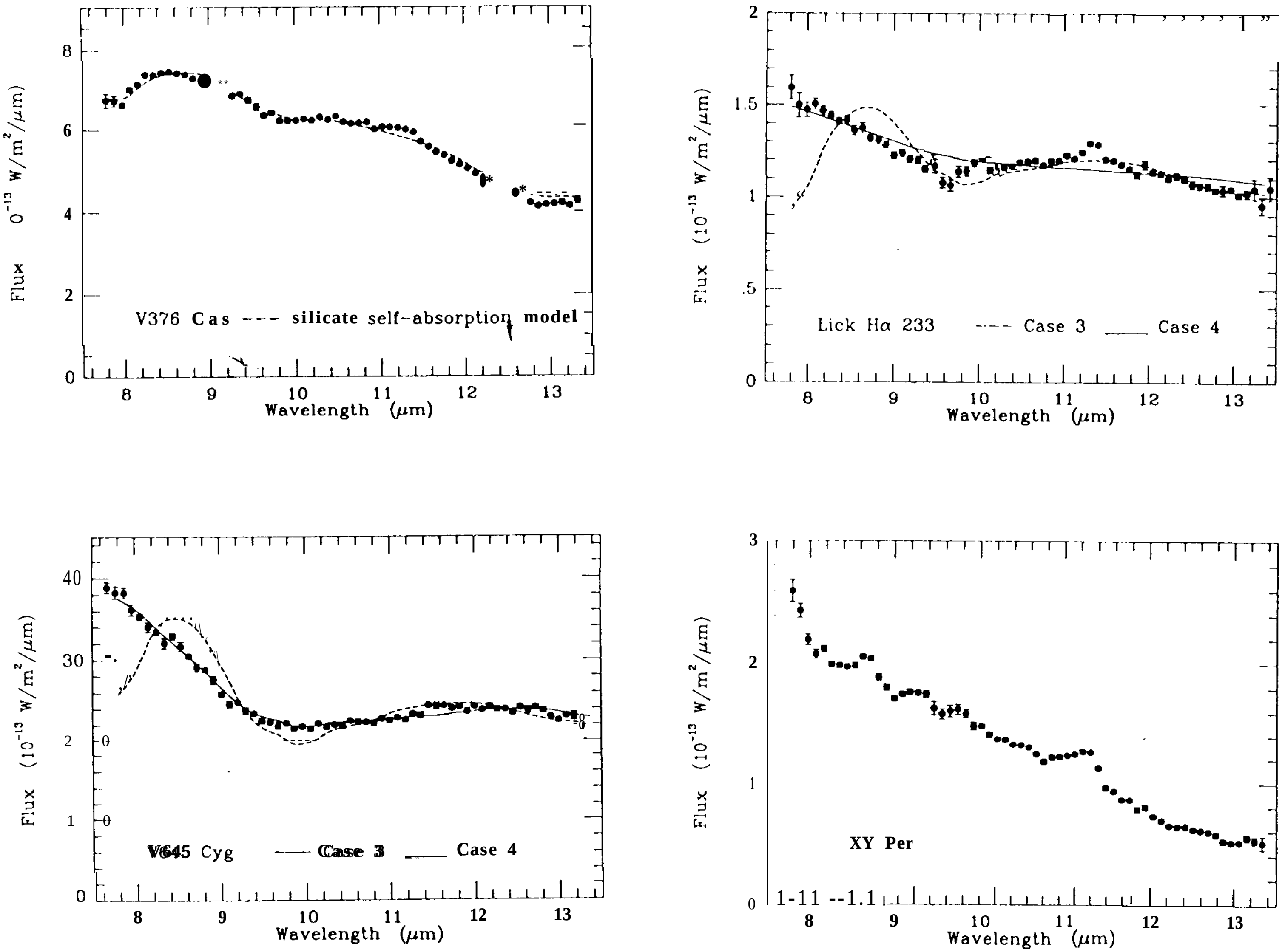
V376 Cas --- silicate self-absorption model
Flux $(10^{-13}$ W/m^2/μm)
Wavelength (μm)
Lick Hα 233
Case 3
Case 4
V645 Cyg
XY Per

Figure 1f-i

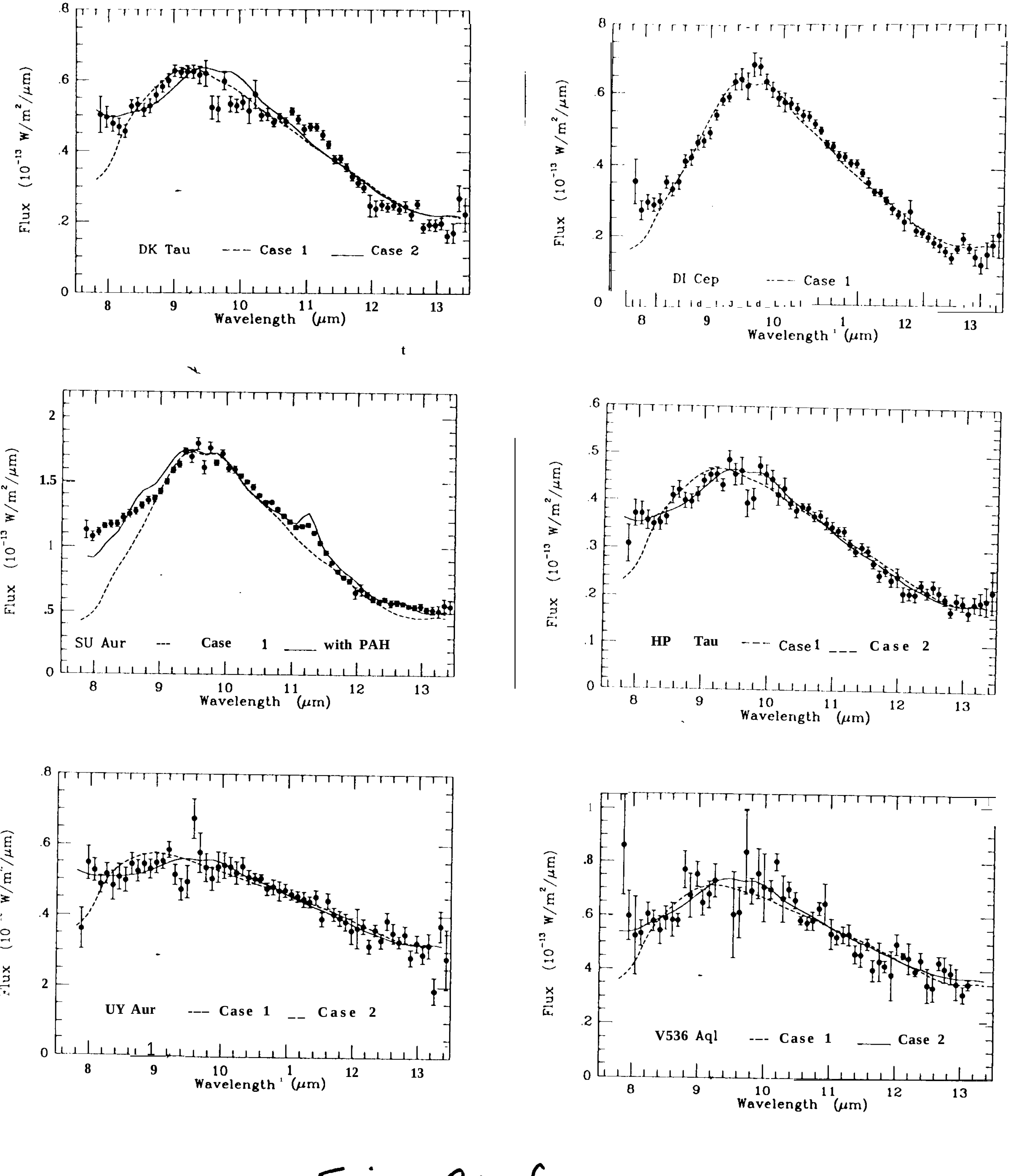
DK Tau --- Case 1 ___ Case 2
DI Cep --- Case 1
SU Aur --- Case 1 ___ with PAH
HP Tau --- Case 1 ___ Case 2
UY Aur --- Case 1 __ Case 2
V536 Aql --- Case 1 ___ Case 2
Flux (10^{-13} W/m^2/μm)
Wavelength (μm)

Figure 2a-f

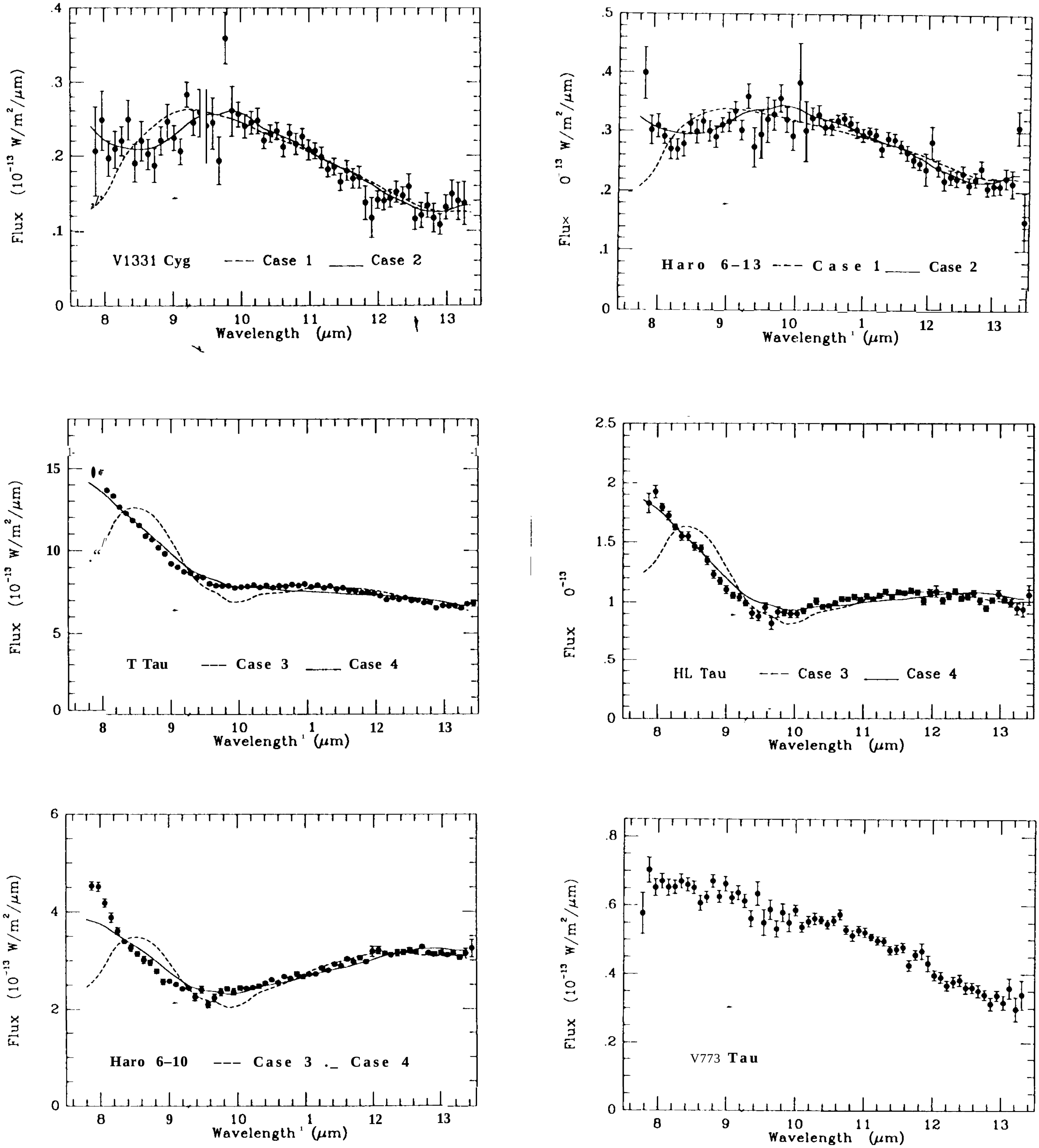
V1331 Cyg --- Case 1 ___ Case 2
Haro 6-13 --- Case 1 ___ Case 2
T Tau --- Case 3 ___ Case 4
HL Tau --- Case 3 ___ Case 4
Haro 6-10 --- Case 3 ._ Case 4
V773 Tau
Flux (10^{-13} W/m^2/μm)
Wavelength (μm)

Fig. 2g-l

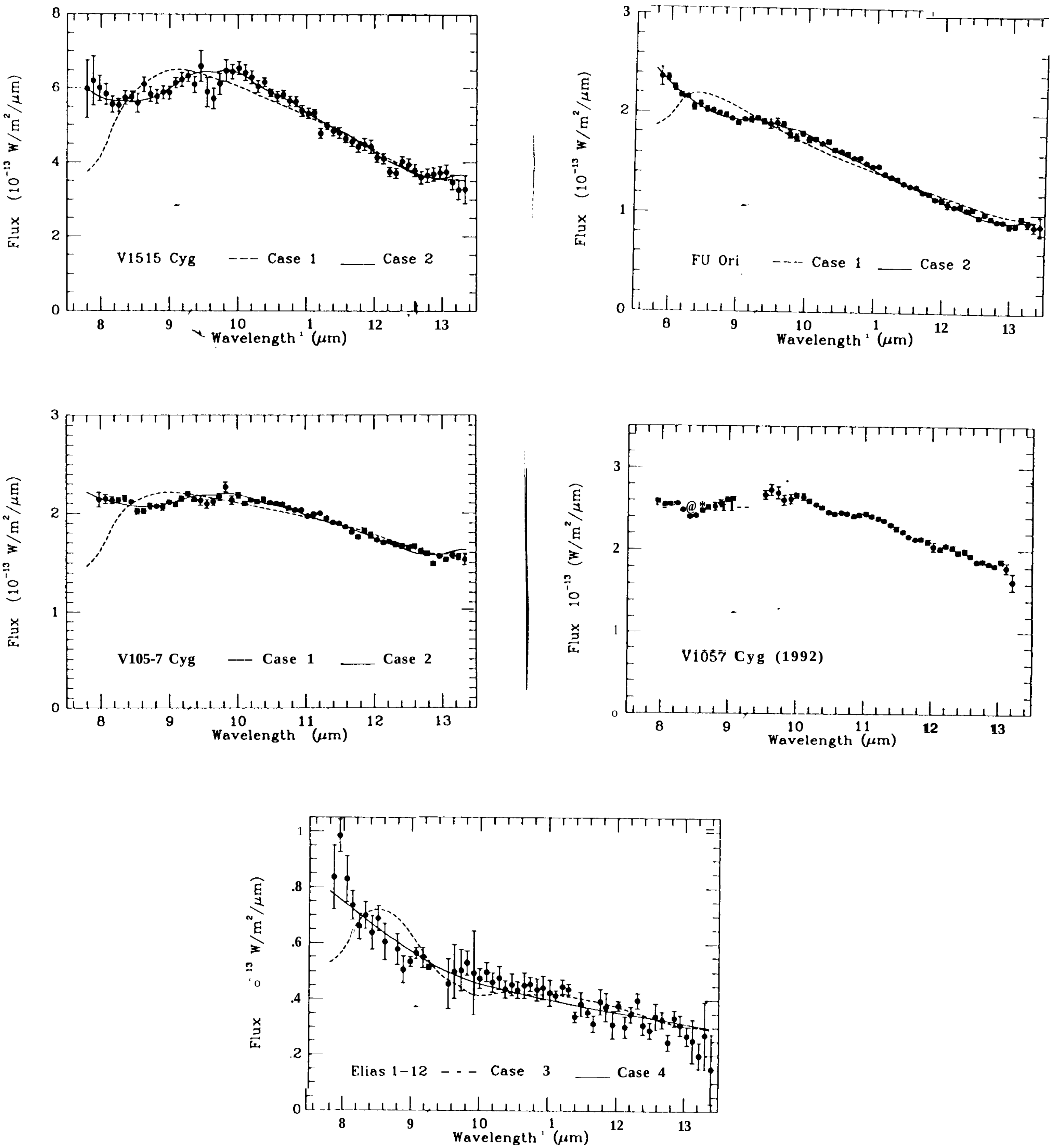
Flux (10^-13 W/m^2/μm)
V1515 Cyg --- Case 1 ___ Case 2
Wavelength (μm)
Flux (10^-13 W/m^2/μm)
FU Ori --- Case 1 ___ Case 2
Wavelength (μm)
Flux (10^-13 W/m^2/μm)
V105-7 Cyg --- Case 1 ___ Case 2
Wavelength (μm)
Flux 10^-13 (W/m^2/μm)
V1057 Cyg (1992)
Wavelength (μm)
Flux 10^-13 W/m^2/μm)
Elias 1-12 --- Case 3 ___ Case 4
Wavelength (μm)

Figure 3

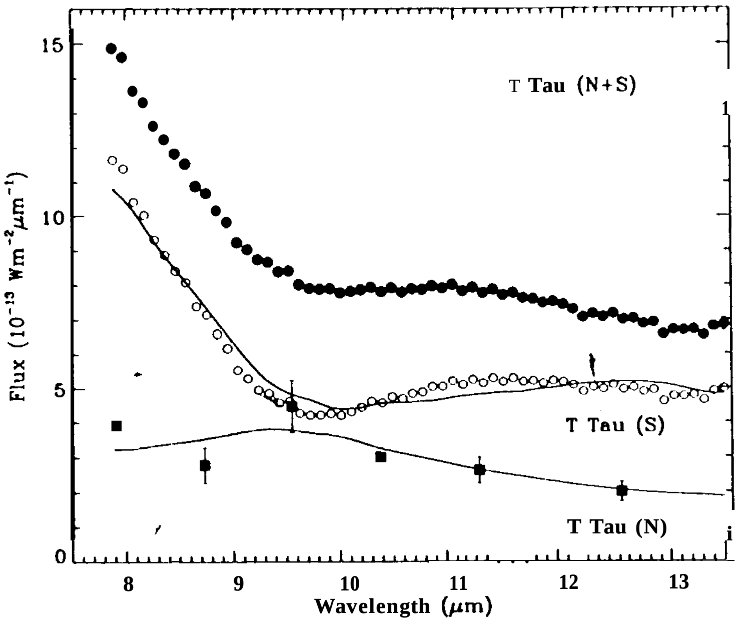

Fig. 4a

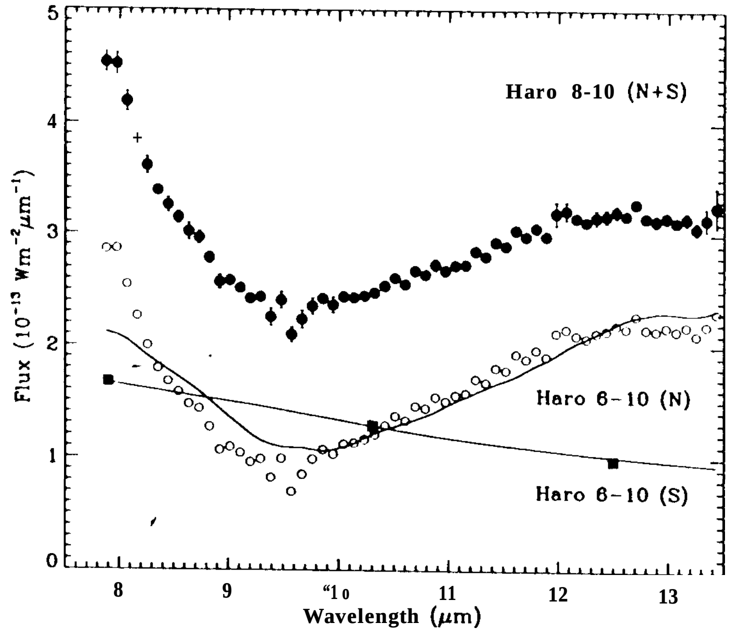

Fig. 4b

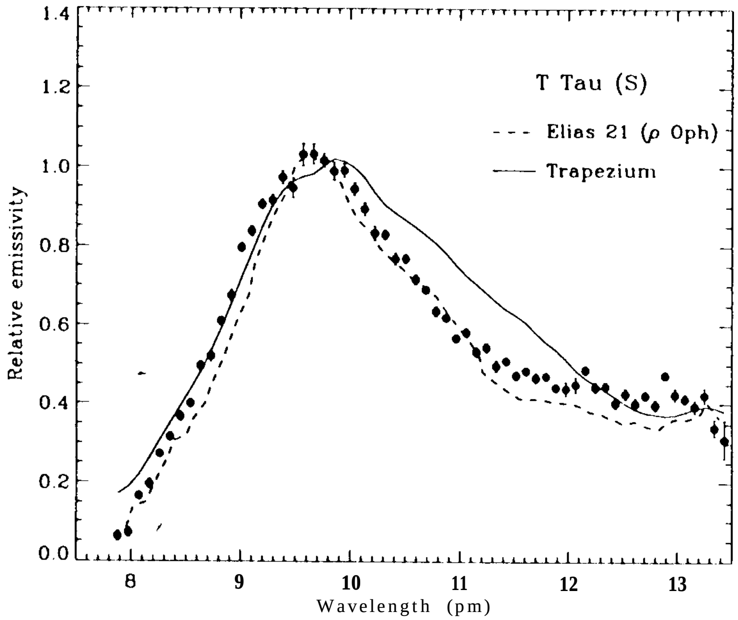

Fig. 5

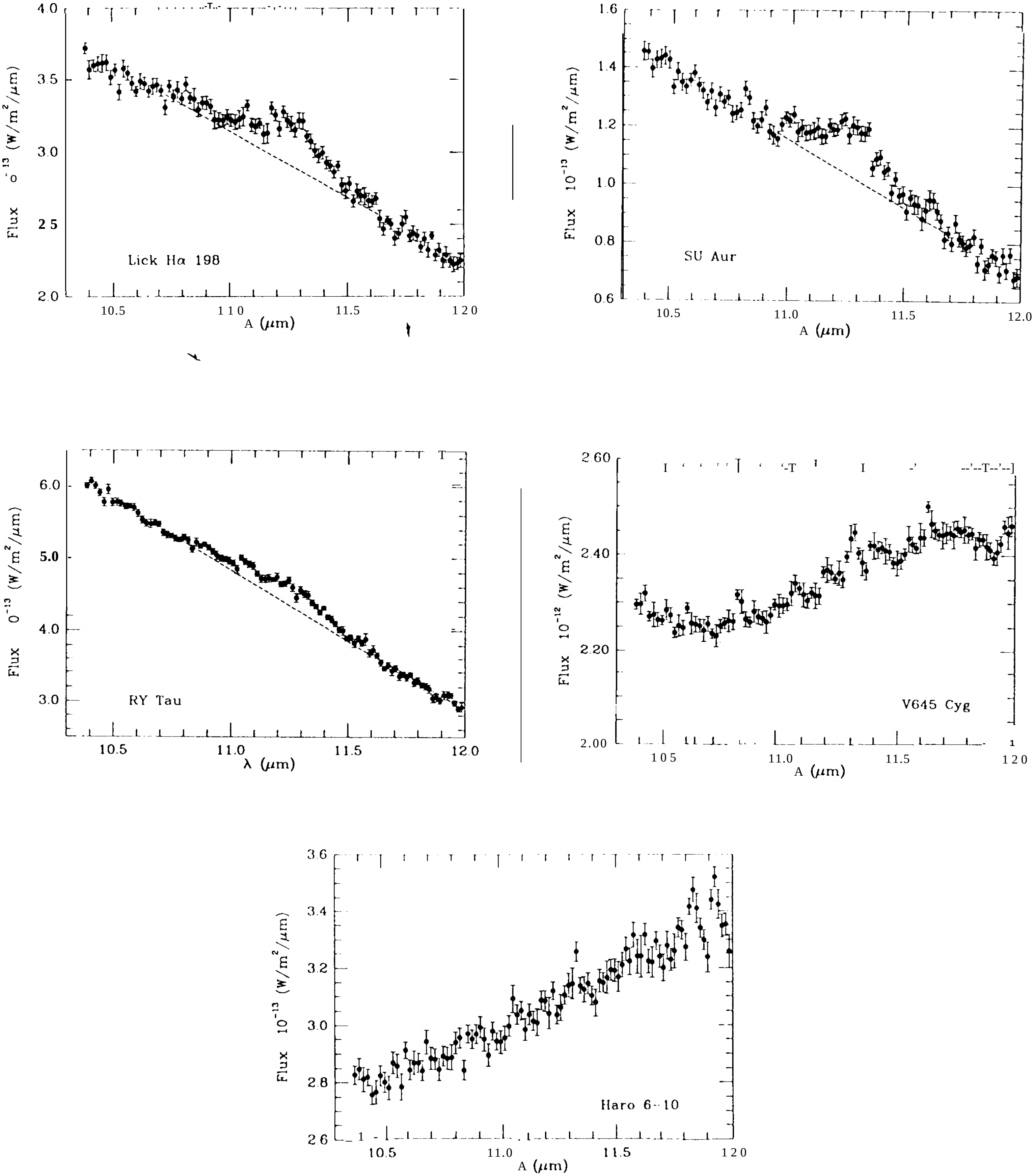
Lick Hα 198
SU Aur
RY Tau
V645 Cyg
Haro 6-10
Flux 10^-13 (W/m^2/μm)
Flux 10^-12 (W/m^2/μm)
λ (μm)

Figure 6

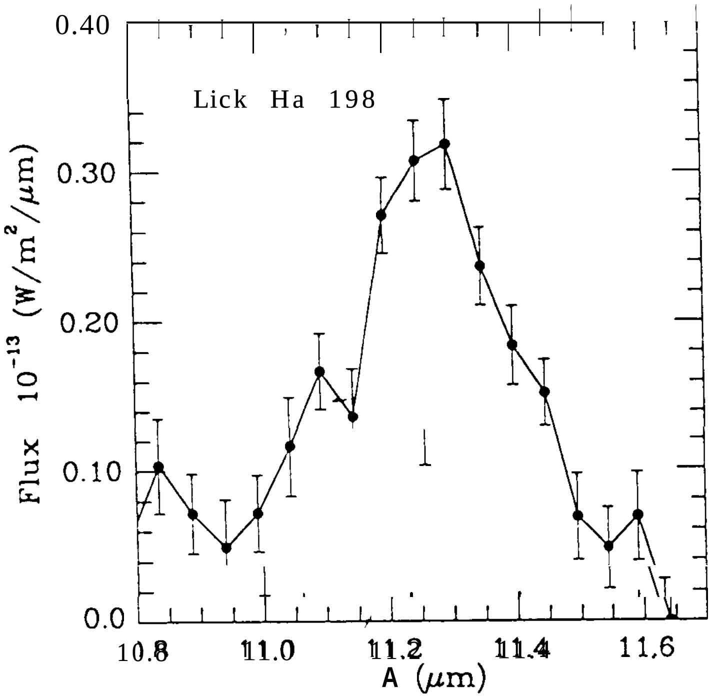

Figure 7

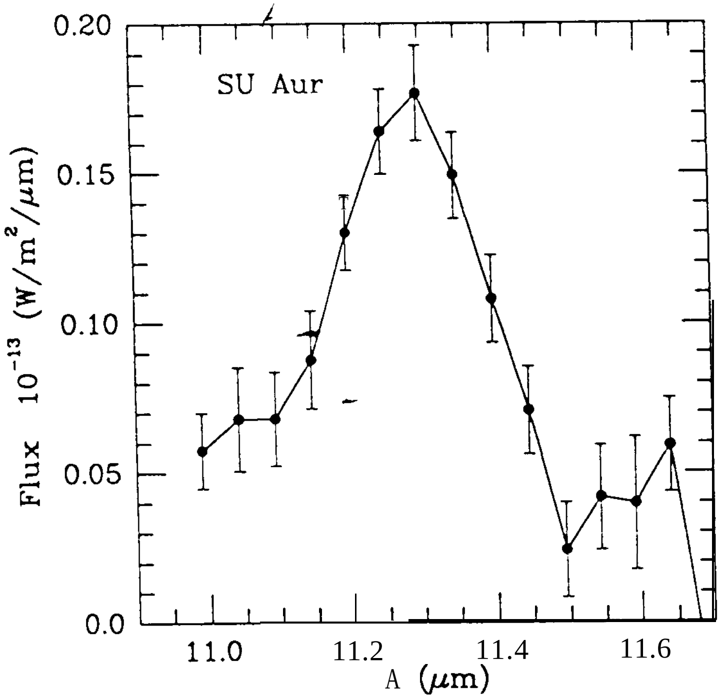

Figure 8